Earth Surf. Dynam. Discuss., doi:10.5194/esurf-2017-34, 2017
Manuscript under review for journal Earth Surf. Dynam.
Discussion started: 19 May 2017

NUMERICAL MODELLING LANDSCAPE AND SEDIMENT FLUX RESPONSE TO PRECIPITATION RATE CHANGE

John J. Armitage[1], Alexander C. Whittaker[2], Mustapha Zakari[1], and Benjamin Campforts[3]

[1]Institut de Physique du Globe de Paris, Université Sorbonne Paris Cité, Paris, France
[2]Department of Earth Science and Engineering, Imperial College London, London, UK
[3]Division Geography, Department of Earth and Environmental Sciences, KU Leuven, Heverlee, Belgium

Correspondence to: John Armitage (armitage@ipgp.fr)

Abstract. Laboratory-scale experiments of erosion have demonstrated that landscapes have a natural (or intrinsic) response time to a change in precipitation rate. In the last few decades there has been a growth in the development of numerical models that attempt to capture landscape evolution over long time-scales. Recently, a sub-set of these numerical models have been used to invert river profiles for past tectonic conditions even during variable climatic conditions. However, there is still an uncertainty over validity of the basic assumption of mass transport that are made in deriving these models. In this contribution we therefore return to a principle assumption of sediment transport within the mass balance for surface processes, and explore the sensitivity of the classic end-member landscape evolution models to change in precipitation rates. One end-member model takes the mathematical form of a kinetic wave equation and is known as the stream power model, where sediment is assumed to be transported immediately out of the model domain. The second end-member model takes the form of a diffusion equation, and assumes that the sediment flux is a function of the water flux and slope. We find that both of these end-member models have a response time that has a proportionality to the precipitation rate that follows a negative power law. For the stream power model the exponent on the water flux term must be less than one, and for the sediment transport model the exponent must be greater than one in order to match the observed concavity of natural systems. This difference in exponent means that sediment transport model responds more rapidly to an increase in precipitation rates, on the order of 10^5 years for a landscape with a scale of $10^5\,\mathrm{m}$. In nature, landscape response times to a rapid environmental change have been estimated for events such as the Paleocene-Eocene thermal maximum (PETM). In the Spanish Pyrenees, a relatively rapid, 20 to 100 kyr, duration of deposition of gravel during the PETM is observed for a climatic shift that is thought to be towards increased precipitation rates. We suggest the rapid response observed is more easily explained through a diffusive sediment transport model, as (1) this model has a faster response time, consistent with the documented stratigraphic data, and (2) the assumption of instantaneous transport is difficult to justify for the transport of large grain sizes as an alluvial bed-load.

1 Introduction

How river networks form and how landscapes erode remains a basic research question despite more than a century of experimentation and study. At a fundamental level, the root of the problem is a lack of an equation of motion for erosion derived

Earth Surf. Dynam. Discuss., doi:10.5194/esurf-2017-34, 2017
Manuscript under review for journal Earth Surf. Dynam.
Discussion started: 19 May 2017

from first principles (e.g Dodds and Rothman, 2000). A range of heuristic erosion equations have however been proposed, from stochastic models (e.g. Banavar et al., 1997; Pastor-Satorras and Rothman, 1998) to deterministic models based on the St. Venant shallow water equations (e.g. Smith and Bretherton, 1972; Izumi and Parker, 1995; Smith, 2010) or the stream power law (e.g. Howard and Kerby, 1983; Whipple and Tucker, 2002; Willett et al., 2014, amongst many others). These models, in various forms, have been explored to try to understand how landscape evolves and responds to tectono-environmental change. In the laboratory, a series of experiments have demonstrated that a change in precipitation rate leads a period of adjustment of the landscape topography until a new steady-state is achieved (e.g. Bonnet and Crave, 2003; Rohais et al., 2011). In this contribution we will focus on this transient period of adjustment to a perturbation in precipitation rates, to evaluate how the response time varies as a function of the model forcing.

It has been increasingly recognised over the last two decades that many basic geomorphic measures of catchments, such as the scaling between channel slopes and catchment drainage areas, are typically unable to distinguish the erosional processes behind their formation (e.g. Tinkler and Whol, 1998; Dodds and Rothman, 2000; Tucker and Whipple, 2002; Whipple, 2004). Erosion and transport can be described by equations that encompass both advective and diffusive processes (e.g. Smith and Bretherton, 1972) and at topographic steady state, it is very well-established that fluvial erosion models based on either of these two end-members can produce very similar river longitudinal profiles (e.g. Tucker and Whipple, 2002; van der Beek and Bishop, 2003).

The morphology of a landscape that is not at topographic steady state relative to the external forcing depends on the magnitude of the advective relative to diffusive processes (Tucker and Whipple, 2002; Godard et al., 2013). If advective processes dominate there is an expectation, based on both numerical models and field studies, that the landscape will respond to a base level fall through the upstream migration of an erosional 'knickpoint' (e.g. Whipple and Tucker, 1999; Snyder et al., 2000; Tucker and Whipple, 2002; Wobus et al., 2006; Whittaker et al., 2008). Topographic responses to a change in precipitation may also include downstream migrating waves of incision and decreases in channel gradient in these cases (e.g. Wobus et al., 2010). These knickpoints can then be inverted for uplift history assuming erosion is a dominantly advective process (e.g Pritchard et al., 2009; Roberts and White, 2010), and more recently including the effect of variable water flux (Goren, 2016).

In contrast, for channels dominated by diffusive processes and perturbed from an initial concave-up steady-state configuration, their longitudinal profiles can maintain a similar shape throughout the adjustment to the new topographic steady state (Whipple and Tucker, 2002; Tucker and Whipple, 2002). The existence of sharp changes in slope along a river profile might therefore be used as evidence that a diffusive transport model is insufficient to explain landscape evolution. However, knickpoints can also be a product of topographic starting conditions (e.g. Valla et al., 2010), a change in lithology (Grimaud et al., 2014, 2016), or formed during extreme events (Baynes et al., 2015), potentially making them a non-unique signal of system erosion. Therefore, there is arguably a need to further explore how both the end-member models respond to change in the forcing conditions to discover how model assumptions control the tempo of landscape response, and how they approximate or approach the real physical system.

Non-uniqueness or equifinality is a common problem when comparing the morphology generated from landscape evolution models (e.g. Hancock et al., 2016). Consequently, we wish to explore if the sediment flux responses of fluvial systems to per-

Earth Surf. Dynam. Discuss., doi:10.5194/esurf-2017-34, 2017
Manuscript under review for journal Earth Surf. Dynam.
Discussion started: 19 May 2017

turbation may also be diagnostically different for the two end-member deterministic models across a range of parameter space. This issue is pertinent because within sedimentary basins, a change in the erosional dynamics upstream could, in principle, be recorded by changes in the total sediment volumes stored in sedimentary basins (e.g. Allen et al., 2013; Michael et al., 2014); in sediment delivery or sediment accumulation rates linked to landscape response times (Foreman et al., 2012; Armitage et al., 2015) and/or in the grain-sizes deposited as a function of sediment flux output (Paola et al., 1992; Armitage et al., 2011; Whittaker et al., 2011; D'Arcy et al., 2016). Furthermore, laboratory scale experiments have demonstrated that within a physical system of erosion dirven by the surface flow of water, there is a clear response time for the system to recover to steady state after a perturbation (Bonnet and Crave, 2003, 2006; Singh et al., 2015).

To date sediment flux response times for the advective stream power law have been previously characterised by Whipple (2001) and Baldwin et al. (2003), although to our knowledge no comparison between the transport model has been previously made. In this article we make a comparative study between the stream power model and the transport model to further explore the potential differences between these two end-member hypothetical landscape evolution models. To this end we aim to find the model parameters that generate similar landscape morphologies such that we can subsequently explore how the same end-member models respond to change in surface run-off. A better understanding of how the landscape evolution models respond to change will allow potentially aid in the interpretation of stratigraphic architecture for past forcing, as it will give an insight as to what processes may be operating within a particular region.

2 Methods

2.1 Erosion within a single dimension system

We wish to understand the effects of the most basic assumptions of mass transport in landscape evolution on the sediment flux record. In other words, how do the response times vary for the advective stream power law and the diffusive sediment transport model? To this end we derive the two models from first principles to demonstrate clearly how, from the same starting point, the fundamental assumptions made about mass transport initially give rise to very different model equations. We use this framework as a context for our investigation of an eroding system responding to precipitation change. We first define a one-dimensional system from which the basic equations can be assembled. Following Dietrich et al. (2003) we define a landscape of elevation z composed of bedrock, thickness η (units of m), and a surface layer of sediment with thickness h (units of m; see Figure 1). This landscape is forced externally through uplift rate U (units of m yr^{-1}). The bedrock is transferred into sediment through erosion at a rate E (units of m yr^{-1}) and the sediment is transported across the system with a flux q_s (units of m^2 yr^{-1}). Assuming that the density of sediment and bedrock are equal, then the change in bedrock thickness is,

$$\partial_t \eta = U - E, \tag{1}$$

and the rate of change in sediment thickness is,

$$\partial_t h = E - \partial_x q_s. \tag{2}$$

Earth Surf. Dynam. Discuss., doi:10.5194/esurf-2017-34, 2017
Manuscript under review for journal Earth Surf. Dynam.
Discussion started: 19 May 2017

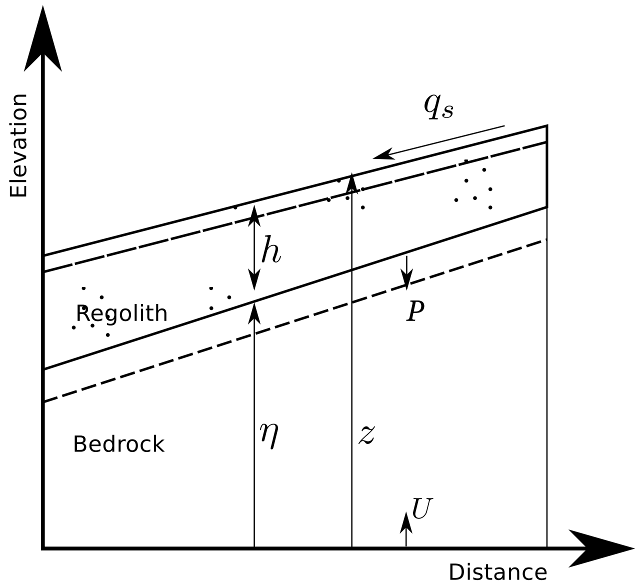

Figure 1. Diagram showing the conservation of mass within a 2-D domain, where mass enters the system through uplift, U (units of $\mathrm{m\,s^{-1}}$), and exists as sediment transported, q_s ($\mathrm{m^2\,s^{-1}}$) out of the domain. P ($\mathrm{m\,s^{-1}}$) is the rate of production of regolith, h (m) is the thickness of regolith, η (m) is the bedrock elevation and z (m) is the total elevation.

It then follows that the rate of change in landscape elevation is,

$$\partial_t z = \partial_t \eta + \partial_t h. \tag{3}$$

It is important to realise that to solve Equation 3, we are required to make some assumptions that fundamentally affect the erosional dynamics of the modelled system, and we illustrate this below. If, and only if, we assume that rate of change in sediment thickness is zero over geological time scales, which is to say all sediment created is transported out of the model domain, than Equation 3 becomes,

$$\partial_t z = U - E. \tag{4}$$

This assumption has been made previously when studying small mountain catchments, where the river may erode directly into the bed-rock. However, recent numerical studies, such as Willett et al. (2014), have expanded this model to cover continent-scale landscapes. Is the assumption of instantaneous mass transport still appropriate at the continent-scale?

It is clearly plausible to suppose that erosion is primarily due to flowing water, so the assumption of geologically instantaneous transport may well be valid for mass that is transported as suspended load within the water column, but such an assumption is less clear for bed-load transport. We can assume that the speed at which suspended loads travel down system is a function of the height achieved within each hop, which is a function of the water depth, settling velocity and flow velocity. For small grains, < 1 mm, the settling velocity is given by the force balance between the weight of the grain and the viscous drag given by Stokes law (Dietrich, 1982). For a particle of diameter 1×10^{-4} m and density $2800\,\mathrm{kg\,m^{-3}}$ the settling velocity is $\sim 0.01\,\mathrm{m\,s^{-1}}$. Therefore the distance traveled assuming a flow velocity of $1\,\mathrm{km\,hr^{-1}}$ and an elevation of suspension of 1 m is roughly 3 km. This distance for the flow velocity and grain size typical of the Bengal Fan is estimated to be $\sim 10^4$ m (Ganti et al., 2014). The percentage of mass transported in suspension may be quite significant. For a small Alpine braided river it was found that the majority of mass was transported as suspended load (Meunier et al., 2006), and for the river systems draining the Tian Shan, China, 70 % of mass is transported as suspended and dissolved load (Liu et al., 2011). Therefore significant mass may be transported rapidly, geologically instantaneously, down system suggesting that the assumption that $\partial_t h \sim 0$ may be valid.

Assuming surface flow is the primary driver of landscape erosion and that positive x is in the downstream direction then erosion, E, as a function of the power of the flow to detach particles of rock per unit width can be written as,

$$E = -k_p \rho_w g q_w^m \left(\partial_x z\right)^n, \tag{5}$$

where k_p is a dimensional constant (units $(\mathrm{m^2\,yr^{-1}})^{1-m}\,\mathrm{yr\,kg^{-1}}$), ρ_w is water density, g is gravity, q_w is water flux per unit width (units $\mathrm{m^2\,yr^{-1}}$), m and n are constants. The exponent $m \sim 0.5$, as it is a function of how the stream flow width is proportional to the water flux (e.g. Lacey, 1930; Leopold and Maddock, 1953; Whittaker et al., 2007). The exponent $n > 0$ acts upon the slope. Using a version of equation 5 to invert river profiles for uplift histories, it is argued by some authors that n is close to unity (Rudge et al., 2015). However, certain river profiles may arguably be indicative of $n > 1$ (Lague, 2014). If $n \neq 1$ equation 5 becomes non-linear.

In two dimensions the change in elevation is then given by,

$$\partial_t z = U + k q_w^m \left(\partial_x z\right)^n, \tag{6}$$

where the constant k lumps together the other constants (units $\mathrm{m^{-1}}\,(\mathrm{m^2\,yr^{-1}})^{1-m}$). To solve this equation in one dimension we assume that the water flux is a function of the precipitation transported down the river network. The water collected is taken from the upstream drainage area, a, which is related to the main stream length, l, by $l \propto a^h$ where h is the exponent taken from the empirical Hack's law (Hack, 1957). The main stream length is related to the longitudinal length of the catchment by, $l \propto x^d$ where $1 \leq d \leq 1.1$ (Tarboton et al., 1990; Maritan et al., 1996). Therefore, we can write that $x \propto a^{h/d}$, and the water flux is the precipitation rate multiplied by the length of the drainage system,

$$q_w = k_w \alpha x^p \tag{7}$$

where k_w is a constant of proportionality (units $\mathrm{m^{1-p}}$), and $p = d/h$. Furthermore, $p < 2$ as it is observed that river catchments are typically elongate (Dodds and Rothman, 2000), and given that $0.5 < h < 0.7$ (e.g. Rigon et al., 1996) then $1.4 < p < 2$. The stream power law for landscape erosion in 1-D is then,

$$\partial_t z = U + k_p \alpha^m x^{mp} \left(\partial_x z\right)^n, \tag{8}$$

where $k_p = k k_w \rho_w g$ (units $\mathrm{m^{-p}}\,(\mathrm{m^2\,yr^{-1}})^{1-m}$).

However, returning to equation 3, we stress that the stream power law is not the only solution if we make a different starting assumption. If we assume that sediment transport is not instantaneous so there is always a supply of transportable sediment, then we can follow through with the summation in equation 3 giving,

$$\partial_t z = U - \partial_x q_s. \tag{9}$$

This may be appropriate when modelling the transport of sediment along the river bed and when considering the formation of alluvial fans (e.g. Whipple and Tucker, 2002; Guerit et al., 2014). In the absence of surface water we can assume that sediment flux is simply a function of local slope $q_s = -\kappa\partial_x z$. In the presence of flowing water then the sediment flux is a function of the flowing water and local slope $q_s = -cq_w^\delta (\partial_x z)^\gamma$ where c is the transport coefficient (units $(\mathrm{m}^2\ \mathrm{yr}^{-1})^{1-n}$), q_w is the water flux per unit width (units $\mathrm{m}^2\ \mathrm{yr}^{-1}$) and the exponents $\delta > 1$ and $\gamma \geq 1$ are dependent on how sediment grains are transported along the bed (Smith and Bretherton, 1972; Paola et al., 1992). Furthermore, $\delta > 1$ is required to create concentrated flow (Smith and Bretherton, 1972). The change in landscape elevation is then given by,

$$\partial_t z = U + \partial_x \left(\kappa\partial_x z + cq_w^\delta (\partial_x z)^\gamma\right). \tag{10}$$

which can be written as,

$$\partial_t z = U + \partial_x \left(\left[\kappa + cq_w^\delta (\partial_x z)^{\gamma-1}\right] \partial_x z\right). \tag{11}$$

Equation 11 is non-linear in the case that $\gamma \neq 1$. In deriving this equation of elevation change due to sediment transport we have simply summed the two terms for sediment flux, the linear and potentially non-linear slope dependent terms. This summation has been done as it is the simplest way to generate landscape profiles that have the desired convex and concave elements observed in natural landscapes (Smith and Bretherton, 1972).

The final step is again to estimate how the water flux changes downstream as the drainage area increases. As before we will assume that $q_w = k_w \alpha x^p$ where $1.4 < p < 2$. Therefore equation 11 becomes,

$$\partial_t z = U + \partial_x \left(\left[\kappa + ck_w \alpha^\delta x^{p\delta} (\partial_x z)^{\gamma-1}\right] \partial_x z\right). \tag{12}$$

We have demonstrated two different fundamental equations for change in elevation in 2-D (equations 6 and 11) and the equivalent 1-D forms (equations 8 and 12). These two models of elevation change differ in that equation 6 is a kinematic wave equation and equation 11 is a diffusion equation. This means that the time evolution of equation 6 would be a migrating wave of erosion traveling either up or down the catchment. This wave could also potentially take the form of a shock-wave, where due to the change in gradient, the lower reaches of the migrating wave could travel faster than the upper reaches, creating a breaking wave (Smith et al., 2000; Pritchard et al., 2009). The time evolution of equation 11 is very different because here the evolution is dominated by diffusive processes. The diffusion coefficient is a function of down-system collection of water, which can lead to the concentration of flow and the creation of realistic morphologies (Smith and Bretherton, 1972), however, the model will respond along the length of the system to change in tecto-environmental forcing.

Earth Surf. Dynam. Discuss., doi:10.5194/esurf-2017-34, 2017
Manuscript under review for journal Earth Surf. Dynam.
Discussion started: 19 May 2017

2.2 Linear and non-linear solutions

If $n = 1$ (equations 6 and 8) and $\gamma = 1$ (equations 11 and 12) then the models are linear, and we can solve the equations both analytically, and in 1-D and 2-D numerical schemes. For the stream power model we use an implicit finite difference scheme (Braun and Willett, 2013) and for the transport model we use an explicit finite element scheme with linear elements (Simpson and Schlunegger, 2003). If $n \neq 1$ and if $\gamma \neq 1$ the equations become non-linear. In this case the numerical solutions can become unstable for simple explicit schemes, and may suffer from too much numerical diffusion for implicit schemes, unless the size of the time step is limited by the appropriate Courant-Friedrichs-Lewy (CFL) condition (Campforts and Covers, 2015). Given the short time steps required to obtain an accurate solution, we explore the non-linear solutions for erosion down a river long profile in 1-D. We solve for the stream power model (equation 8) using an explicit total variation diminishing scheme with the appropriate CFL condition (Campforts and Covers, 2015). For the transport model (equation 12) we use an explicit finite element model with quadratic elements and the appropriate CFL condition to find a stable solution.

2.3 Generalizing to a two dimensional system

To solve equations 6 and 11 over a 2-D domain requires an algorithm to route surface flow down the landscape. In our case, to explore how a model landscape responds to change in uplift and precipitation rate we will make the simplest assumption available; that water flows down the steepest slope. We then solve for equation 6 using the numerical model Fastscape (Braun and Willett, 2013), with a resolution of 1000 by 1000 nodes for a 100 by 100 km domain, giving a spatial resolution of 100 m. Erosion by sediment transport is solved following the methods of Simpson and Schlunegger (2003). We solve Equation 11 on a triangular grid with a resolution of 316 by 316 nodes for a 100 by 100 km domain, giving a spatial resolution of the order of 300 m. The time step used for both models is 10 kyrs.

To explore the response of the two models to change in precipitation rate we start the model with a precipitation rate of $1\,\mathrm{m\,yr^{-1}}$ for a duration of 5 or 10 Myr. The precipitation rate is then either reduced or increased to a new value for a duration of 5 or 10 Myr. As the coefficients k and c have units that are related to the exponents m and δ in equations 6 and 11 respectively (e.g. Whipple and Meade, 2006; Armitage et al., 2013), when modelling increasing values of m and δ the coefficients are likewise increased.

The response time for the sediment transport model scales by the effective diffusivity, and can be given by,

$$\tau_t = \frac{L^2}{\kappa + c q_w^\delta} \tag{13}$$

where L is the model length scale (in this case the length of the domain). For the stream power model the response time is a function of the velocity at which the kinematic wave travels up the catchment (e.g. Whipple and Tucker, 1999; Whipple, 2001). The response time is therefore given by the time it takes for this wave of incision to travel up the catchment length, l_c,

$$\tau_{sp} = \frac{l_c}{k q_w^m} \tag{14}$$

Therefore we expect the response time to be a function of the choice of both the constants c and k, and the exponents δ and m within both models. The effect of varying the coefficients m and δ independently has been previously explored (e.g.

Earth Surf. Dynam. Discuss., doi:10.5194/esurf-2017-34, 2017
Manuscript under review for journal Earth Surf. Dynam.
Discussion started: 19 May 2017

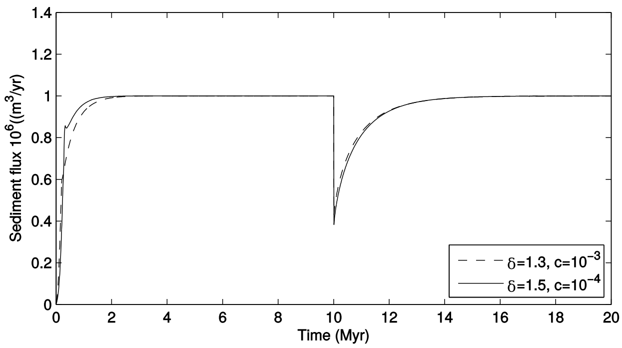

Figure 2. Sediment flux out of the sediment transport model for a step reduction in precipitation from 1 to $0.5\,\mathrm{m\,yr^{-1}}$ after 10 Myr. Two models are plotted, where $\delta = 1.3$ and 1.5, $\kappa = 10^{-2}$ and $c = 10^{-3}$, and $10^{-4}\,(\mathrm{m^2\,yr^{-1}})^{1-\delta}$.

Whipple and Meade, 2006; Armitage et al., 2013), and we therefore will not do so in detail again here. Instead we wish to compare the two models, and therefore search for the values of c, k, m and δ that generate similar topography at steady state. This steady state is then perturbed by a change in precipitation rate.

We will explore how an idealized landscape evolves under uniform uplift at a rate of $0.1\,\mathrm{mm\,yr^{-1}}$. The initial condition is of a flat surface with a small amount of noise added to create a roughness. The boundary conditions are of fixed elevation at the left and right sides, and of no flow at the sides.

3 Results

It has been previously demonstrated that both end-member models can generate convex-up long profiles (e.g. Kirkby, 1971; Smith and Bretherton, 1972; Smith et al., 2000; Whipple and Tucker, 2002; Crosby et al., 2007). From solving both equations 8 and 12 where $n = 1$ and $\gamma = 1$ we find that in range $0.3 \leq m \leq 0.7$ and $1 < \delta \leq 1.5$ the two end-member models are comparable (see Appendix A). Given the possible additional degree of freedom introduced if we also vary n and γ, it is clear that river-long profiles are not a unique identifier of erosional process. However, in order to compare how the end-member models respond to change in precipitation rate, it is preferable to perturb catchments of a similar morphology. The stream power and sediment transport model can both fit observed slope-area relationships of the present day landscape morphology within a certain parameter range ($m \sim 0.5$ or $\delta \sim 1.5$; see Appendix B). Therefore, both models may be a reasonable representation of how, on a gross scale, a landscape erodes. We therefore fix the slope exponents at these values and explore how the models, in their linear and non-linear forms, respond to a change in precipitation rates.

3.1 Response to precipitation rate reduction

In Figure 2 we display the response of erosion for the sediment transport model, in terms of sediment flux out of the model domain, for a reduction in precipitation rate from 1 to $0.5\,\mathrm{m\,yr^{-1}}$ at 10 Myr of model evolution. We explore how the transport

Earth Surf. Dynam. Discuss., doi:10.5194/esurf-2017-34, 2017
Manuscript under review for journal Earth Surf. Dynam.
Discussion started: 19 May 2017

Table 1. Response to change in precipitation rate where α_1 is value the precipitation rate changes to from $\alpha_0 = 1\,\mathrm{mm\,yr^{-1}}$. Response time is given for two model sizes, 100 and 500 km, and as the time for the model to recover by half and a tenth towards the steady state sediment flux.

$L = 100\,\mathrm{km}$	transport		detachment	
α_1	$\tau_{1/2}$	$\tau_{1/10}$	$\tau_{1/2}$	$\tau_{1/10}$
$\mathrm{mm\,yr^{-1}}$	Myr	Myr	Myr	Myr
0.25	1.42	6.07	0.98	1.66
0.50	0.53	2.19	0.70	1.18
0.75	0.30	1.21	0.57	0.98
2.00	0.09	0.31	0.34	0.60
$L = 500\,\mathrm{km}$	transport		detachment	
α_1	$\tau_{1/2}$	$\tau_{1/10}$	$\tau_{1/2}$	$\tau_{1/10}$
$\mathrm{mm\,yr^{-1}}$	Myr	Myr	Myr	Myr
2.00	0.17	0.64	0.34	0.60

model responds for $\delta = 1.5$, $c = 10^{-4}$; $\delta = 1.3$, $c = 10^{-3}$ as these two values of δ generate resonable slope area relationships (Figure 13b). The response to a reduction in precipitation is very similar with the flux initially reducing by a half and then recovering to within 10 % of steady state values within ∼2 Myr (Figure 2; see Table 1). Changing the transport coefficient, c, does not affect predicted slope area relationship (Appendix A); importantly, however, it changes the model elevation, larger c creates more transport and it alters the model response time: the larger the value of c the faster the response (Equation 13; see Armitage et al., 2013). Response is slower for smaller values of δ, therefore the increase in c counters this effect, and for the values chosen both models respond at a similar rate to the change in precipitation.

The response of the stream power model to an identical reduction in precipitation at a model time of 10 Myr takes a similar form, with an initial decease in sediment flux out followed by a gradual recovery (Figure 3). In a similar manner as the transport model, response is a function of the exponent m and the coefficient k (Equation 14). We have modeled three parameter sets: $m = 0.3$ and $k = 10^{-4}$, $m = 0.5$ and $k = 10^{-5}$, and $m = 0.7$ and $k = 10^{-6}$. Response time to achieve return to 10 % of the steady state sediment flux varies from 3 Myr in the case of $m = 0.3$ to less than 1 Myr when $m = 0.7$. As well as response time being longer for smaller values of m, the peak magnitude of the flux response is reduced for smaller values of m (Figure 3).

The magnitude of the response for all the runs is greater for the sediment transport model when compared to the stream power model (Figures 2 and 3). Consequently, response time, while being a function of the transport coefficients c and k respectively, may still systematically differ between the two models: The sediment transport model with $\delta = 1.5$ and $c = 10^{-4}$ generates a maximum model elevation of $\sim 240\,\mathrm{m}$, and the stream power model with $m = 0.5$ and $k = 10^{-5}$ generates a maximum elevation of $\sim 180\,\mathrm{m}$. These two models have a similar slope area relationship at steady state (Table 3) and are

Earth Surf. Dynam. Discuss., doi:10.5194/esurf-2017-34, 2017
Manuscript under review for journal Earth Surf. Dynam.
Discussion started: 19 May 2017

Earth Surface Dynamics
Discussions
Open Access

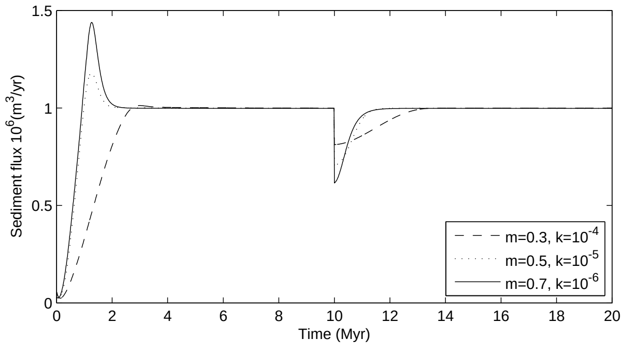

Figure 3. Sediment flux out of the stream power model for a step reduction in precipitation from $\alpha_0 = 1\,\mathrm{m\,yr^{-1}}$ to $\alpha_1 = 0.5\,\mathrm{m\,yr^{-1}}$ after 10 Myr. Three models are plotted, where $m = 0.3$, 0.5 and 0.7, and $k = 10^{-4}$, 10^{-5}, and $10^{-6}\,\mathrm{m^{-1}\,(m^2\,yr^{-1})^{1-m}}$.

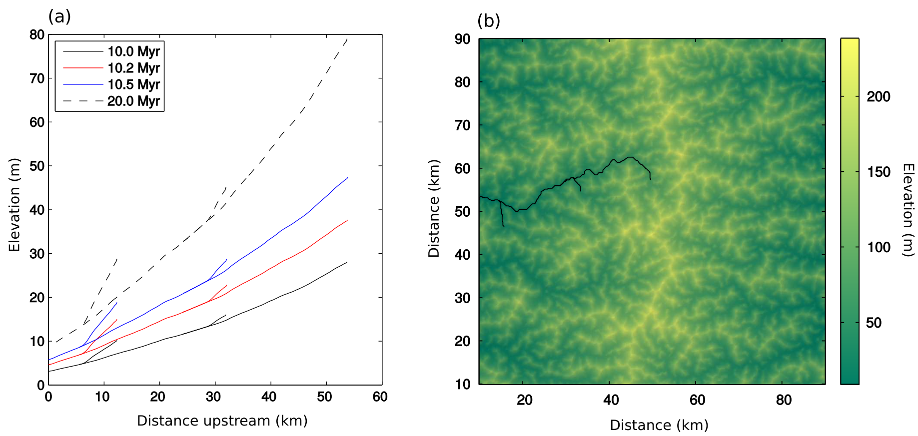

Figure 4. Transport model evolution due to a reduction in precipitation. (a) Selected river long profile response to change in precipitation. Black line is the profile just before a factor of two reduction in precipitation. The red and blue lines are 200 kyr and 500 kyr after the reduction in precipitation. The dashed black line is the steady state profile. (b) Trunk stream used for the analysis with the steady state elevation.

therefore comparable suggesting a faster response to a reduction in precipitation rates for the stream power model (Figures 2 and 3).

To explore how the difference in response time and magnitude is expressed in the landscape, we extract the river profiles of the main trunk systems for models where $\delta = 1.5$ and $m = 0.5$ during the responce to the reduction in precipitation rate while uplift rate is constant (Figures 4 and 5). For the sediment transport model in which $\delta = 1.5$ and $c = 10^{-4}$, the catchment elevation increases to a new steady state that has an elevation that is roughly 2.6 times higher than the steady state elevation after 10 Myr (Figure 4). Just under half of this new topographic elevation is achieved within the first 500 kyr, and the increase in elevation occurs without any knickpoint migration. In contrast, for the stream power model where $m = 0.5$ and $k = 10^{-5}$, the steady state topography is achieved within a fraction of the time when compared to the transport model ($\sim 500\,\mathrm{kyr}$). This is

Earth Surf. Dynam. Discuss., doi:10.5194/esurf-2017-34, 2017
Manuscript under review for journal Earth Surf. Dynam.
Discussion started: 19 May 2017

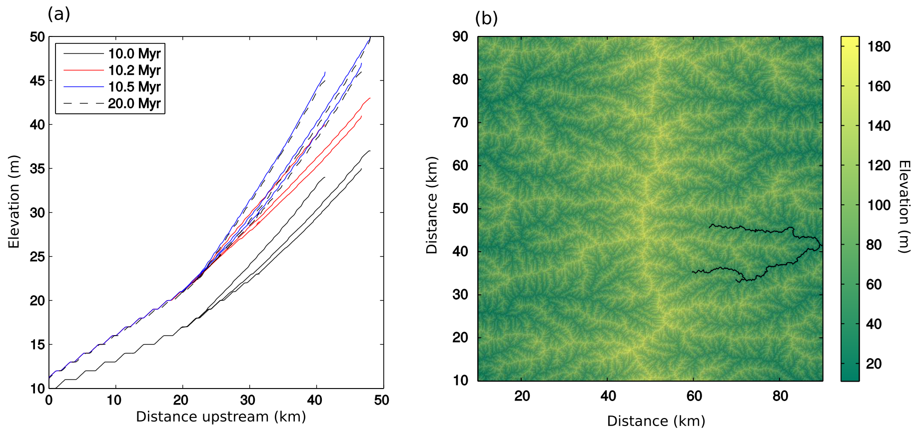

Figure 5. Stream power model model evolution due to a reduction in precipitation. (a) Selected river long profile response to change in precipitation. Black line is the profile just before a factor of two reduction in precipitation. The red and blue lines are 200 kyr and 500 kyr after the reduction in precipitation. The dashed black line is the steady state profile. (b) Trunk stream used for the analysis with the steady state elevation.

in line with the more rapid response of this model to a relative drying of the climate using these parameters (compare Figures 2 and 3). Furthermore the increase in elevation due to the reduced surface water flux is only a factor of ~ 1.2, which is less than half of the increase for the sediment transport model. The lower reaches of the catchment respond more rapidly than the upper reaches, therefore creating a migrating knickpoint as the landscape responds to the change in model forcing (see Braun et al., 2015).

3.2 Response timescales to different magnitudes of precipitation rate change

Our results confirm that two different end-member erosion models, encompassing advective and diffusive mathematics can produce landscapes with similar morphologies, if particular parameter sets are selected accordingly. However the key question here is whether these landscapes produce different sediment flux responses if perturbed from their steady state configuration, and if so, how do they differ in magnitude and timescale? The response time of the sediment transport model is known to be a function of the transport coefficient and the magnitude of the precipitation rate (c.f. Armitage et al., 2013). This behavior is displayed in Figure 6a, where the response of the transport model with $\delta = 1.5$ and $c = 10^{-4}$ for a change in precipitation from 1 to 0.25, 0.5, 0.75 and $2\,\mathrm{m\,yr^{-1}}$ is plotted. The response time measured as the time for the sediment flux to recover by half and by 90 % to the steady state value is shown additionally in Figure 7 as black solid and dashed lines respectively and in Table 1. For a reduction to $0.25\,\mathrm{m\,yr^{-1}}$ the prediction is for a long response time of 6.07 Myr, while for an increase to $2\,\mathrm{m\,yr^{-1}}$ the prediction is a for rapid response time of 310 kyr for 90 % recovery towards previous sediment flux values. The equivalent half life, recovery by 50 % towards previous sediment flux values, is 1.42 Myr and 90 kyr.

The stream power model likewise has a response time that is a function of precipitation rate (Figure 6b). For a reduction to $0.25\,\mathrm{m\,yr^{-1}}$ the prediction is for a response time of 1.66 Myr, while for an increase to $2\,\mathrm{m\,yr^{-1}}$ the prediction is for recovery

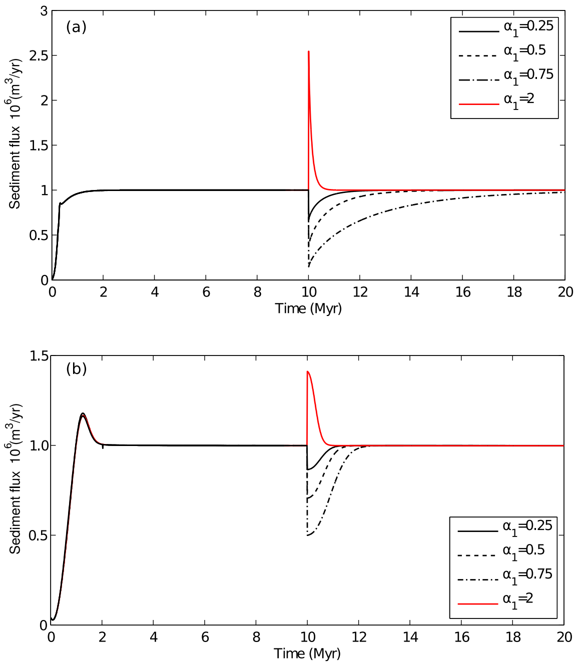

Figure 6. (a) Response of the sediment transport model to change in precipitation rate. Equation 11 is solved for $\delta = 1.5$ and $c = 1 \times 10^{-4}\,(\mathrm{m^2\,yr^{-1}})^{1-\delta}$. The precipitation rate is initially $\alpha_0 = 1\,\mathrm{m\,yr^{-1}}$ and changes to $\alpha_1 = 0.25$, 0.5, 0.75 or $2\,\mathrm{m\,yr^{-1}}$ after 10 Myr. (b) Response of the stream power model to change in precipitation rate. Equation 11 is solved for $m = 0.5$ and $k = 1 \times 10^{-5}\,\mathrm{m^{-1}}\,(\mathrm{m^2\,yr^{-1}})^{1-\mathrm{m}}$. The precipitation rate is initially $\alpha_0 = 1\,\mathrm{m\,yr^{-1}}$ and changes to $\alpha_1 = 0.25$, 0.5, 0.75 or $2\,\mathrm{m\,yr^{-1}}$ after 10 Myr.

time of 600 kyr for 90 % recovery (Table 1). The equivalent half life is 0.98 Myr and 340 kyr (Table 1). The stream power model is therefore faster to recover for a reduction in precipitation rate yet slower for an increase in precipitation rate. This is because the response time of the stream power model is more weakly a function of precipitation rate. Importantly, these results therefore suggest there is a fundamental asymmetry in the response timescale to a climate perturbation, in which a drying event takes much longer to recover from, compared to wetting events.

Both models display a response time that is a function of the precipitation rate (Figures 6 and 7). Given that for the models $q_w = \alpha l_d$, where l_d is the drainage network length, the relationship between precipitation rate and the sediment transport model response can be expressed as,

$$\tau_t \propto \alpha^{-\delta} \tag{15}$$

where in this case $\delta = 1.5$. This proportionality is in agreement with our numerical model results, where the slope of trend for the sediment transport model in the log-log plot is -1.5 (Figure 7).

In contrast, the response time of the stream power model is not as strongly inversely dependent on the precipitation rate (Figure 7). For this model, the response time is a function of the velocity at which the wave of incision travels up-stream, and

Earth Surf. Dynam. Discuss., doi:10.5194/esurf-2017-34, 2017
Manuscript under review for journal Earth Surf. Dynam.
Discussion started: 19 May 2017

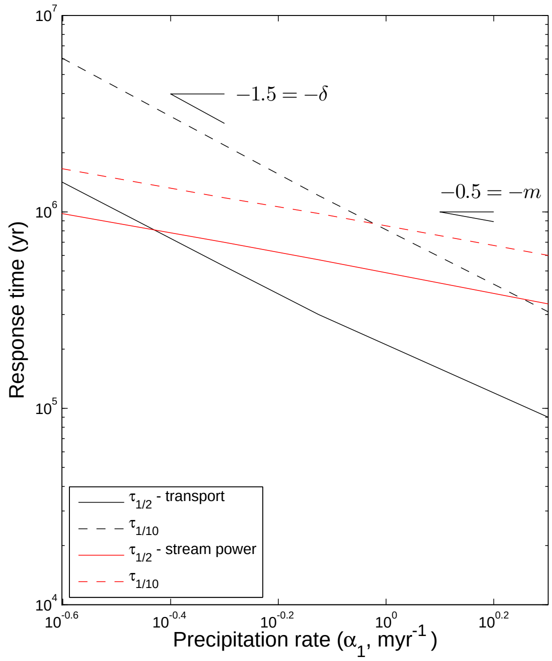

Figure 7. Log-log plot of response time to change to a precipitation rate α_1 from an initial value of $\alpha_0 = 1\,\mathrm{m\,yr^{-1}}$ (see Table 1). $\tau_{1/2}$ is the time for the sediment flux to recover by a half of the magnitude change in sediment flux and $\tau_{1/10}$ is the time for the sediment flux to recover by 90 %.

the portion of the channel downstream of the knock-point provides the locus of enhanced erosion. This velocity is directly related to the inverse of the water flux, q_w^m, which is in turn again a function of the drainage length and precipitation rate, α. Therefore for the stream power model we can write that response time is,

$$\tau_{sp} \propto \alpha^{-m}. \tag{16}$$

This proportionality, which is in agreement with the approximate analytical solutions of Whipple (2001), is likewise in agreement with our numerical model results, where the slope of trend for the stream power model in the log-log plot is -0.5 (Figure 7). Consequently, for these two models, which were derived from the same starting point (Figure 1), and applied to catchments of similar topography and morphology, we find that above a certain magnitude of precipitation rate change, the sediment transport model responds more rapidly than the stream power model and vice versa.

The position of the critical point where the stream power model responds more rapidly than the sediment transport model is a function of the water flux and the collection of coefficients. In the model comparison developed here, we have compared two model catchments that have similar concavity, β between 0.4 and 0.5 ($\delta = 1.5$ and $m = 0.5$) and model domain length of $L = 100\,\mathrm{km}$ giving catchments of roughly 50 km length. In this case the 90 % recovery of the sediment flux signal is

Earth Surf. Dynam. Discuss., doi:10.5194/esurf-2017-34, 2017
Manuscript under review for journal Earth Surf. Dynam.
Discussion started: 19 May 2017

predicted to be more rapid for the sediment transport model when compared to the detachment limited model for an increase in precipitation rate (Figure 7). If however the model domain is increased to $L = 500\,\mathrm{km}$ then a 90 % recovery takes twice as long to recover from an increase in precipitation rate from 1 to $2\,\mathrm{m\,yr^{-1}}$: 0.63 Myr compared to 0.31 Myr for $L = 100\,\mathrm{km}$ (Table 1). This recovery time is now similar to the equivalent stream power model where $m = 0.5$, which remains 0.60 Myr.

The stream power model is insensitive to the size of the model domain because of the particular choice of m and the shape of drainage network that forms under the assumptions of routing water down the steepest slope of descent. Taking the drainage length to be directly proportional to the catchment area, $l_d \propto a$, and given that catchment length is proportional to drainage area raised to the Hack exponent, h, we can re-write equation 14 as,

$$\tau_{sp} \propto \frac{a^h}{(\alpha a)^m}. \quad (17)$$

Therefore, in the case that $h = 0.5$ and $m = 0.5$, as in the numerical model here, the response time becomes independent of system length (c.f. Whittaker and Boulton, 2012). If $h < m$ then response times would reduce with increasing drainage basin size, and if $h > m$ then response times would increase with drainage basin size. There is good empirical evidence for $0.5 < h < 0.7$ (e.g. Rigon et al., 1996), yet there is not a complete consensus on the value of m (see Lague, 2014; Temme et al., 2017).

A final key difference between the transient sediment flux responses of the two models is that the peak magnitude of system response to a change in precipitation rate is systematically larger for the sediment transport model (Figure 6). For an increase in precipitation rates from 1 to $2\,\mathrm{m\,yr^{-1}}$, the sediment flux increases from $1 \times 10^6\,\mathrm{m^3}$ to $2.5 \times 10^6\,\mathrm{m^3}$ for erosion by sediment transport. This is three times greater than the equivalent increase for the stream power model. The reduction in sediment flux is likewise larger for the sediment transport model (Figure 6). Therefore, although response time is a function of precipitation rate, the magnitude of change is consistently larger for the sediment transport model.

3.3 Non-linear response timescales

Up to this point we have compared how the models respond to a precipitation rate change when the solutions are linear. However, there is reasonable debate as to the value of the slope exponent n in the stream power model (e.g. Lague, 2014; Croissant and Braun, 2014; Rudge et al., 2015) and likewise within the transport model it is plausible that the slope exponent $\gamma > 1$. The response time for the stream power model for various values of n has been explored within Baldwin et al. (2003). Here we expand on this by exploring the equivalent response times for the transport model. To explore the implications of the non-linearity introduced by relaxing the constraint that $n = 1$ and $\gamma = 1$ for both models, we solve equations 8 and 12 for $p = 1.1$, $m = 0.5$, $k = 10^{-4}$ and $\delta = 1.5$ and $c = 5 \times 10^{-5}$ respectively with different uplift rates. We have modelled the response due to an uplift rate of between 0.1 and $1.0\,\mathrm{mm\,yr^{-1}}$ for the case where $n = 1.2$ and $\gamma = 1.2$ in equations 8 and 12 (Figure 8).

We find that for both the transport and stream power model, when the slope exponent is greater than one the model response time is a function of uplift rate. The faster the rate of uplift the faster the system responds to a change in precipitation rate. If the response time for a system recovery to steady state by 50 % or 10 % is plotted on a log-log plot against uplift rate we find

Earth Surf. Dynam. Discuss., doi:10.5194/esurf-2017-34, 2017
Manuscript under review for journal Earth Surf. Dynam.
Discussion started: 19 May 2017

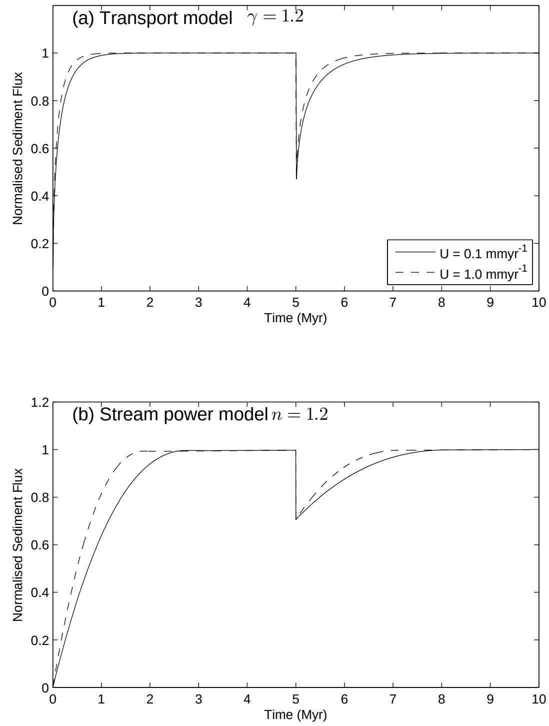

Figure 8. (a) Response of the sediment transport model to change in precipitation rate for two values of uplift, 0.1 and $1.0\,\mathrm{mm\,yr^{-1}}$. Equation 12 is solved for $\gamma = 1.2$, $\delta = 1.5$, $p = 1.1$ and $c = 5 \times 10^{-5}\,(\mathrm{m^2\,yr^{-1}})^{1-\delta}$. The precipitation rate is initially $\alpha_0 = 1\,\mathrm{m\,yr^{-1}}$ and changes to $\alpha_1 = 0.5$. (b) Response of the stream power model to change in precipitation rate for two values of uplift, 0.1 and $1.0\,\mathrm{mm\,yr^{-1}}$. Equation 8 is solved for $n = 1.2$, $m = 0.5$, $p = 1.1$ and $k = 1 \times 10^{-4}\,\mathrm{m^{-1}}\,(\mathrm{m^2\,yr^{-1}})^{1-\mathrm{m}}$. The precipitation rate is initially $\alpha_0 = 1\,\mathrm{m\,yr^{-1}}$ and changes to $\alpha_1 = 0.5$ after 5 Myr.

that the response time is proportional to the uplift rate raised to a negative power (Figure 9). In the case of $n = 1.2$ or $\gamma = 1.2$ the slope of trend is -0.1667, and for $n = 2$ or $\gamma = 2$ the slope of trend is -0.5 (Figure 9). These slopes are in agreement with the approximate analytical solutions of Whipple (2001) and numerical models of Baldwin et al. (2003), i.e. the stream power response time τ_{sp} has a proportionality,

$$\tau_{sp} \propto U^{\frac{1}{n}-1} \tag{18}$$

and equivalently we infer from our numerical model (Figure 9) that the transport limited response time as,

$$\tau_t \propto U^{\frac{1}{\gamma}-1}. \tag{19}$$

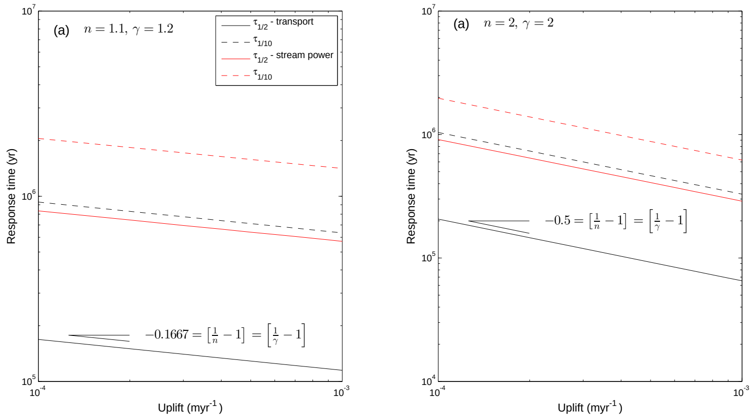

Figure 9. Log-log plot of response time for different slope exponents and uplift rates to change to a precipitation rate from an initial value of $\alpha_0 = 1\,\mathrm{m\,yr^{-1}}$ to $\alpha_0 = 0.5\,\mathrm{m\,yr^{-1}}$. $\tau_{1/2}$ is the time for the sediment flux to recover by a half of the magnitude change in sediment flux and $\tau_{1/10}$ is the time for the sediment flux to recover by 90 %. (a) Response time for the transport model (equation 12) and stream power model (equation 8) when the slope exponent $\gamma = 1.2$ and $n = 1.2$ respectfully. A linear trend is found with a gradient of -1.667. (b) Response time for the transport model and stream power model when the slope exponent $\gamma = 2$ and $n = 2$ respectfully. A linear trend is found with a gradient of -0.5.

This implies that both models have the same form of response dependency on uplift rates, and regardless of the rate of uplift we should expect the transport model to respond more rapidly to a large increase in precipitation rate and the stream power model to respond more rapidly to a reduction in precipitation rate.

4 Discussion

4.1 Response times

Under certain parameter sets it is relatively straightforward to generate two landscapes, eroded by diffusive or advective mathematics that have similar elevation, slope and area metrics (Appendix B). To find a path to break the apparent non-unique solutions we have explored the response in terms of sediment flux out of the model domain for two end-member solutions to erosion. The first observation is that both models respond in a broadly similar way to a precipitation rate (climate) driver (Figure 7). Both models have a response that is an inverse function of the magnitude of precipitation rate change. Both models have a response that is related to uplift in an identical manner (Figure 9). However, the responses for catchments that are comparable in slope-area relationship and maximum elevation, but which are governed by different erosional dynamics defined by c, k, m and δ, actually display different response times by almost one order of magnitude.

We have demonstrated that models limited by their ability to transport sediment tend to have shorter response times to an increase in rainfall rate, and thus re-achieve pre-perturbation sediment flux values more rapidly compared to stream power dominated systems when catchment length-scales are small (e.g. < 100 km, Figure 7). The trend in response is asymmetric, by which we mean that both models show a faster response for a precipitation increase relative to a precipitation decrease. Given that the the response time is a function of the water flux exponent (m or δ), and that the water flux exponent for the sediment transport model is greater than that for the stream power model, there will be a cross over point where the stream power model responds faster than the transport model. This cross-over point is a function of the erodability coefficient k and the transport coefficient c. In the scenario where we have tried to initiate the perturbation in precipitation rates from similar catchments, we find that this cross-over point is towards large reductions in precipitation rates (Figure 7). This implies that the sediment transport model generally responds faster than the stream power model, when the parameters produce similar landscapes.

The stream power model predicts a landscape response time to a change in precipitation of the order of 10^6 yr, and this time is related to the precipitation rate to the inverse power of m (Figure 7). Furthermore this time scale is not sensitive to catchment length (Table 1). The sediment transport model predicts a wider range of response times of order 10^6 to 10^5 yr that is related to the precipitation rate to the inverse power of δ, also in this case the response time is length dependent (Figure 7 and Table 1). It has been suggested that a transition from a landscape controlled by detachment-limited erosion to sediment transport at longer system lengths may explain the longevity of mountain ranges (Baldwin et al., 2003). This hypothesis is somewhat backed up by the analysis of response times for the sediment transport model, as the response time increases with system length (Table 1) unlike the stream power model, which has a response that is only slightly modified by system length (Whipple, 2001; Baldwin et al., 2003).

4.2 Relevance of model responses to sediment records of climate change

To what extent do these model results help us to understand how stratigraphic records of sediment accumulation through time do, or do not, reflect the effects of climatic change on sediment routing systems governed by differing long-term erosional dynamics?

One motivation for this study came from a number of field and stratigraphic investigations of terrestrial sedimentary deposits contemporaneous with known past climate perturbations, such as the Palaeocene Eocene thermal maximum (PETM), a hyperthermal event that occurred around 56 Ma. The PETM is arguably the most rapid global warming event of the Cenozoic, with a rise in global surface temperatures by 5 to 9 °C (Dunkley Jones et al., 2010). The initial warming associated with this event may have been abrupt as 20 kyr, with a duration of 100 to 200 kyr based on synthesis of δ13C and δ18O records (e.g. Foreman et al., 2012). The event has been associated with clear changes to global weather patterns, for instance hydrogen isotope reocrds suggest increased moisture delivery towards the poles at the onset of the PETM, consistent with predictions of storm track migrations during global warming (Sluijs et al., 2006). This event has also been argued by a number of authors to have produced a significant geomorphic and erosional impact based on sedimentary evidence, and its apparent effect on the global hydrological cycle and catchment run-off (e.g. Foreman et al., 2012; Foreman, 2014).

At the onset of the PETM there is strong evidence for the contemporaneous increase in precipitation rates and the deposition of coarse gravels, ranging from the Claret Conglomerate (Schmitz and Pujalte, 2007), in the Tremp Basin of the Spanish Pyrenees to the well-documented channel sandstone bodies in the Piceance Creek and Bighorn Basins, western USA

Earth Surf. Dynam. Discuss., doi:10.5194/esurf-2017-34, 2017
Manuscript under review for journal Earth Surf. Dynam.
Discussion started: 19 May 2017

(Foreman et al., 2012; Foreman, 2014, e.g.). In the US cases, the deposits include coarse channelized sands, marked by upper flow regime bed forms, which are consistent with a synchronous increase in both water and sediment discharge. At Claret, the conglomerate has a thickness of $\sim 10\,\mathrm{m}$ while the total carbon isotope excursion (CIE) in the same section measures $\sim 35\,\mathrm{m}$ (Manners et al., 2013). If we assume a constant rate of deposition, then the conglomerate accounts for roughly 30 % of the total duration of deposition for the CIE (90 to 170 kyr; Röhl et al., 2007), suggesting deposition occurred over a duration of 25 to 50 kyrs. If we however drop the simple assumption of constant accumulation, and assume that the sediment accumulated at a rate of c.a. $5 \times 10^{-4}\,\mathrm{m\,yr^{-1}}$, in line with lower accumulation rates from paleosols within the Bighorn Basin during the PETM (e.g. Bowen et al., 2001), then the duration for the deposition of paleosols at Claret is $\sim 70\,\mathrm{kyr}$. This leaves a duration of conglomeratic deposition at between 25 and 70 kyr. Therefore unless there is a major unconformity within the CIE, the implication is that the erosional system responded rapidly, in less than 100 kyr to a significant shift in climatic conditions.

Erosional source catchment areas were likely < 100 km in length at the time, given the palaeo-geography of the Pyrenees at the time (Manners et al., 2013). The very short duration of the depositional response, coupled with the extensive deposition of gravel clasts within a mega-fan setting in which sediment was clearly abundant is difficult to model or explain within an advective end-member model (e.g. Table 1). In contrast, the model of sediment transport more easily reproduces the documented response timescales given an increase in precipitation, is consistent with the export of bedload transported gravel clasts, and therefore honors the independent field data more effectively. The time-equivalent sections in the Bighorn and Piceance Creek basins of the western US (Foreman et al., 2012; Foreman, 2014) also provide clear evidence of anomalous sedimentation at the PETM, in this case with a somewhat longer duration of $> 200\,\mathrm{kyrs}$. However, the basin responses, including the deposition of coarse sand bodies, are clearly longer than the CIE associated with the PETM event, suggesting a more complex relationship between increased precipitation and the export of volumetrically significant coarse sediments. Our approach evidently does not reproduce complex dynamics such as vegetation turn-over and sediment reworking that may influence large-scale stratigraphic responses and we note the relative difficulty of reliably reconstructing climatic and hydrological variables from geologic data in the past makes it challenging to compare field outputs directly and unambiguously with models that illustrate end-member responses. Furthermore, it is possible that the system response is sensitive to the initial condition assumed for the landscape (e.g. Perron and Royden, 2012).

For the sediment transport model, it has been previously demonstrated that an increase in the transport coefficient c will reduce the model response time predictably (Armitage et al., 2013). The erodability parameter k has a similar effect for the stream power model. In this paper we have attempted to find the values of c, k, m and δ that generate comparable model landscapes, and then changed the precipitation rate to understand the form of the model response. Above we discussed the geological relevance of the models with such a choice of c, k, m and δ, yet of course both models could have the values of their transport coefficient or erodability adjusted further to tune them to the observations. Furthermore, while inverse models suggest that the slope exponent $n \sim 1$ (e.g. Rudge et al., 2015), there is room for argument over the non-linear nature of the fundamental equations (see Harel et al., 2016). Therein lies the rub of these heuristic models, and the potential difficulties in arguing for the applicability of one over the other. However, we note that the transport model does display a response time that has a stronger dependence on precipitation rate change. Furthermore, in the Spanish Pyrenees the PETM shift in

Earth Surf. Dynam. Discuss., doi:10.5194/esurf-2017-34, 2017
Manuscript under review for journal Earth Surf. Dynam.
Discussion started: 19 May 2017

climatic conditions is recorded as a short duration deposition of gravels down-system. The transport of such large clasts is most likely in the form of bed-load movement, which conceptually is more easily described by transport equations rather than the instantaneous stream power model.

5 Conclusions

Deterministic numerical models of landscape evolution rest on fundamental assumptions on how sediment is transported down system. The kinematic wave equation that is the stream power law is based on the assumption that all sediment generated is transported instantaneously out of the landscape. Sediment transport models assume that there is an endless supply of sediment to be transported. The existence of knickpoints within river long profiles, assumed to be produced by a system pertubation such as a base level, has been used to provide evidence in support of the stream power law in upland areas (e.g. Whipple and Tucker, 1999; Snyder et al., 2000; Whittaker et al., 2008). Knickpoints however can likewise be a result of changes in lithology (Grimaud et al., 2014; Roy et al., 2015) and are certainly not a unique indicator of erosion dynamics (e.g. Tucker and Whipple, 2002; Valla et al., 2010; Grimaud et al., 2016). In this contribution we therefore attempted to understand of the sediment flux signal out of the eroding catchment may generate a distinguishable difference between the end-member models in term of a response to a change in run-off. This idea is motivated from field observations of past landscape responses to climate excursions, such as the PETM, which are manifested in the rapid deposition of coarse sedimentary packages in terrestrial depocentres (Armitage et al., 2011; Foreman et al., 2012).

Both models suggest that the response time of landscape to change in precipitation rate has a proportionality of the form of a negative power law (equations 15 and 16). The key difference is in the value of the exponent. For the stream power model, the exponent must be less than one in order to match the observed concavity of river profiles. In contrast, for the transport model the exponent on the precipitation rate must be greater than one in order to generate a river network (Smith and Bretherton, 1972), and to generate the observed concavity of river profiles. This results in the sediment transport model responding more rapidly to an increase in precipitation rate in comparison to the stream power law model (Figure 7). Additionally, our results show that there is a fundamental asymmetry in the response of the transport limited models to a climatic perturbation, with the response time to a drying event longer than that to an increase in rainfall. In general terms, the magnitude of the response to a change in precipitation rate appears greater across the range of model space investigated here for the sediment transport (diffusive) model solutions, while for the stream power (advective) model, the magnitude of the sediment flux perturbation is smaller, but is more localised within the catchment with respect to knickpoint retreat.

While our models obviously do not address whether or not these sediment flux signals will be preserved in the stratigraphic record, a problem that fundamentally rests on the availability of accommodation to capture the eroded sediment (c.f. Allen et al., 2013), it does suggest that landscapes governed by these simple erosional end-members should be sensitive to climate change; and moreover that there are some important diagnostic differences between their sediment flux responses to an identical perturbation. Using published stratigraphic examples, we suggest that the timescales and magnitude of coarse sediment deposition in the Spanish Pyrenees at the time of the PETM are best described using the transport limited end-member, while other examples are more equivocal. Consequently, we argue that these model end-members allow us to constrain the range of likely sediment flux scenarios that precipitation changes may generate, and that numerical models, in conjunction with a range of field and independently-constrained proxy data sets are best placed to tease apart when and in what circumstances climate signals are likely to have been generated and preserved in sedimentary systems.

6 Code availability

The codes developed here are available from John Armitage (armitage@ipgp.fr). Fastscape is available from Jean Braun (GFZ Potsdam) by request.

Appendix A: Steady state 1-D profiles

The solution to the one dimensional stream power law (Equation 8) assuming that at the end of the catchment at $x = L$ elevation $z = 0$ and $mp \neq 1$ is,

$$z_{sss} = \frac{U}{mk\alpha^m (mp-1)} \left(x^{(1-mp)} - Lx^{(1-mp)} \right) \tag{A1}$$

and for the case where $mp = 1$ this simplifies to,

$$z_{sss} = \frac{U}{k\alpha^m} log_e(L/x) \tag{A2}$$

For the sediment transport model (Equation 12) there is an exact solution for the case that $\delta p = 2$, which assuming at $x = 0$, $\partial_x z = 0$ and at $x = L$, $z = 0$ is,

$$z_{sst} = -\frac{UL}{2\kappa D_e} \left(log(D_e x^2 + 1) + log(D_e + 1) \right) \tag{A3}$$

where,

$$D_e = \frac{ck_w \alpha^{2/p} L^2}{\kappa}. \tag{A4}$$

For other values of δp the steady state solution is solved for numerically, where Equation 12 is solved using the finite element method with linear weight functions. We use a non-uniform 1-D nodal spacing, where the spatial resolution is increased with increasing gradient. The numerical model is bench-marked against the analytically solution for the case where $np = 2$.

The steady state solutions are plotted in the case that $\delta = p = \sqrt{2}$ and for reference the stream power model solution with $m = 0.5$ and $p = \sqrt{2}$ (Figure 10). Such a value of p assumes that $h \sim 0.7$, which is towards the higher end for observed Hack exponents and that the river catchment is very elongate. When plotting the logarithm of the model slope against drainage area (Figure 10b), where area is given by $a = x^p/k_w$ and assuming $k_w = 1$, for the simple stream power law derived here the gradient $\beta = -m$. The value of the dimensional constant k has no impact on the gradient as expected. The sediment transport model likewise creates river long profiles that have on average a negative curvature. For small values of x there is however a

Earth Surf. Dynam. Discuss., doi:10.5194/esurf-2017-34, 2017
Manuscript under review for journal Earth Surf. Dynam.
Discussion started: 19 May 2017

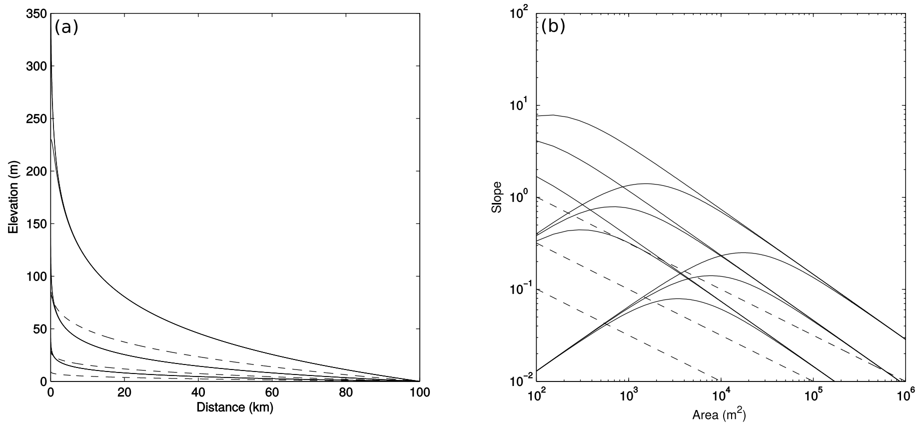

Figure 10. Steady state profiles of elevation against down-system length, and the slope of the profile plotted against the drainage area assuming that area $a = x^p$ where $p = 1/h = \sqrt{2}$ and h is the Hack exponent. Solid lines are for the stream power law (Equation 8) with $m = 0.5$, and $k = 10^{-4}$, $10^{-3.5}$, and 10^{-3}. The dashed lines are for the sediment transport model (Equation 12 with $n = \sqrt{2}$, $\kappa = 10^{-3}$, 1 and $10^3\,\mathrm{m^2\,yr^{-1}}$, and $c = 10^{-6}$, $10^{-5.5}$, and 10^{-5}.

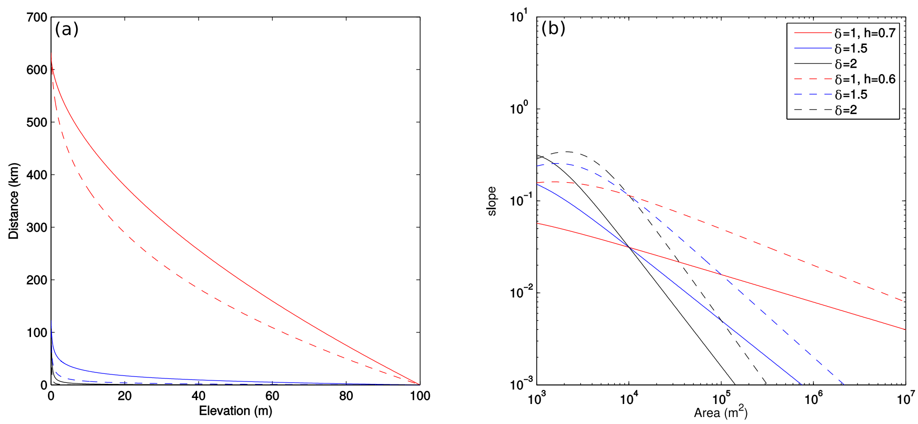

Figure 11. Steady state elevation and slope-area relationship for the numerical solution to 1-D sediment transport (Equation 12), where the area, a, is taken to be related to distance x by $a = x^p$ where $p = 1/h$ and h is the Hack exponent. Red lines are for the case where $n = 1$, blue lines for $n = 1.5$ and black lines for $n = 2$. Solid lines are for $h = 0.7$. Dashed lines are for $h = 0.6$.

region of positive curvature where $\kappa > ck_w\alpha^\delta L^{\delta p}$. For the slope area analysis this leads in there being a positive gradient in the trend for small catchment areas. This relationship subsequently has a negative slope for larger catchments. The point of inflection is dependent on the value of D_e, where for smaller values of κ the region of positive gradient is reduced. There is therefore a critical catchment area that is dependent on the diffusive term κ. After this critical point the slope area relationship becomes negative. At distances down-system, where the upstream area is greater than this critical area, the gradient $\beta = -0.88$. β is insensitive to the coefficient c as would be expected.

Table 2. Gradient, β, of the slope vs. area trend at steady state for 1-D sediment transport (Equation 12, Figure 11).

δ	$p = 1.40$		$p = 1.67$		$p = 2.00$	
	c	β	c	β	c	β
1	10^{-6}	-0.50	10^{-5}	-0.40	10^{-4}	-0.30
1.5	10^{-8}	-1.01	10^{-7}	-0.91	10^{-6}	-0.81
2	10^{-10}	-1.51	10^{-9}	-1.41	10^{-8}	-1.31

The range of gradients found for river catchments for this type of slope area analysis, usually referred to as concavity, generally lies within the range $\beta = -0.35$ to -0.70 (Snyder et al., 2000). It is trivial to find the values of m for the steady state solution to the stream power law such that fits such values of β. To further explore how β depends on δ and p within the sediment transport model we solve Equation 12 numerically for $\delta = 1$, 1.5 and 2 while keeping $h = 0.7$ or 0.6 (Figure 11). The result is that β varies from -0.3 for the case of $\delta = 1$ to -1.31 for $\delta = 2$. The values of the gradient for the slope area analysis for $1.4 < p < 2$, where we are assuming $d = 1$ and hence $p = 1/h$, are displayed in Table 2. For the sediment transport model the slope is dependent on both δ and p.

Clearly there exists a combination of δp that is equally capable of fitting the observed river long profile. Furthermore, for the sediment transport model the slope is a function of the Hack exponent h (and therefore p) and the choice of δ. This because of the diffusivity term that leads to positive curvature and rounded 1-D profiles (Figure 10b and 11). The magnitude of the water flux term within the transport equation (Equation 12) is dependent on how much water the river network captures, which is in turn a function of how elongated the catchment is. For this reason, the slope area relationship is sensitive to the river network geometry for the diffusive case, while for the simple stream power relationship it is not.

The positive slope area relationship for the transport model for small catchment area, see Figure 10b and 11b, has been previously explored in Willgoose et al. (1991). In the study of Willgoose et al. (1991) the governing equations were however of a significantly greater complexity. For realistic catchment areas, for the sediment transport model the gradient of the slope area analysis (concavity) is dominantly a function of the exponent δ within Equation 11. The value of this exponent has been assumed to be within the range of $1 < \delta < 2$ depending on the bed-load transport law assumed (Armitage et al., 2013). If the observations of trunk river slope against catchment area are representative of a landscape at steady state then for the smaller range of $1 < \delta \leq 1.5$ a realistic catchment topography can be generated.

Appendix B: Idealized linear 2-D models

B1 Erosion by Sediment Transport

We explore how an idealized landscape evolves under uniform uplift at a rate of $0.1\,\mathrm{mm\,yr^{-1}}$ for the case in which erosion is dependent on sediment transport. The initial condition is of a flat surface with a small amount of noise added to create a roughness. The boundary conditions are of fixed elevation at the left and right sides, and of no flow at the sides. The sediment

Earth Surf. Dynam. Discuss., doi:10.5194/esurf-2017-34, 2017
Manuscript under review for journal Earth Surf. Dynam.
Discussion started: 19 May 2017

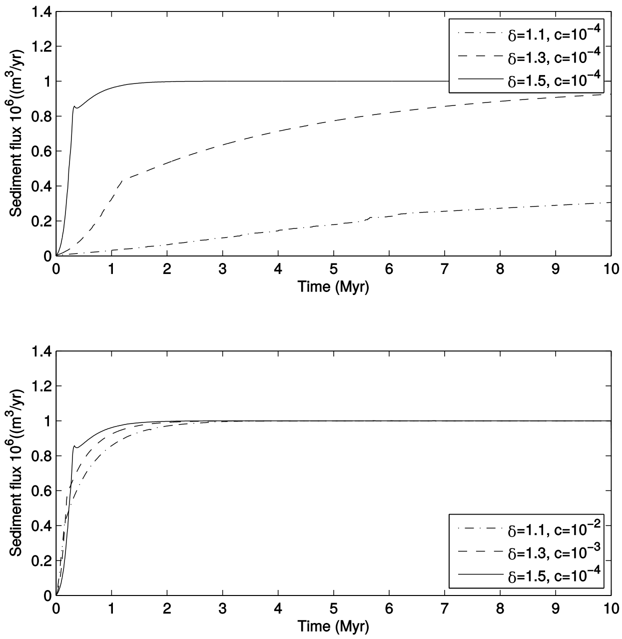

Figure 12. Sediment flux out of the model domain for the sediment transport model for models where (a) $\delta = 1.1$, 1.3 and 1.5, $\kappa = 10^{-2}$ and $c = 10^{-4}\,(\mathrm{m^2\,yr^{-1}})^{1-\delta}$, and (b) $\delta = 1.1$, 1.3 and 1.5, $\kappa = 10^{-2}$ and $c = 10^{-2}$, 10^{-3}, and $10^{-4}\,(\mathrm{m^2\,yr^{-1}})^{1-\delta}$.

flux output is displayed in Figure 12. Six models have been run without a change in precipitation to find the steady state topography. The models explored are first a set of three with varying δ and constant c, i.e.; $\delta = 1.1$, 1.3 and 1.5 with $c = 10^{-4}\,(\mathrm{m^2\,yr^{-1}})^{1-\delta}$ (Figure 12a), and a set of three where δ and c co-vary, i.e.; $\delta = 1.1$ with $c = 10^{-2}\,(\mathrm{m^2\,yr^{-1}})^{1-\delta}$, $\delta = 1.3$ with $c = 10^{-3}\,(\mathrm{m^2\,yr^{-1}})^{1-\delta}$, and $\delta = 1.5$ with $c = 10^{-4}\,(\mathrm{m^2\,yr^{-1}})^{1-\delta}$ (Figure 12b).

When the transport coefficient c is the same for the three values of the exponent δ the model wind-up time increases with decreasing δ, and takes several million years where $\delta < 1.5$ (Figure 12a). Steady state sediment flux is greater for increasing δ when c is kept constant. The dimensions (units) of c depend on δ which means that the value of the coefficient c must be adjusted when δ is changed to yield the same unit erosion rate per water flux, regardless of δ (see Armitage et al., 2013). Consequently, when c is suitably adjusted the model can reach a steady state in a similar time for all three values of δ (Figure 12b).

We subsequently analyze the topography for the relationship between trunk river slope and drainage area, Figure 13, using Topotoolbox2 (Schwanghart and Scherler, 2014). For the case where $\delta = 1.5$ the scaling between channel slopes and catchment drainage areas, slope area gradient, β is equal to -0.42, and for $\delta = 1.3$, β is equal to -0.23 (Figure 13b). The same value is calculated using the spatial transformation described within (Perron and Royden, 2012), commonly referred to as χ-plots (Table 3). Given the reduction in β from $\delta = 1.5$ to 1.3, we did not analyze the case for $\delta = 1.1$ as the slope-area relationship will clearly lie below the observed range ($0.3 < \beta < 0.7$; e.g. Whipple and Tucker, 2002; Tucker and Whipple, 2002). Therefore,

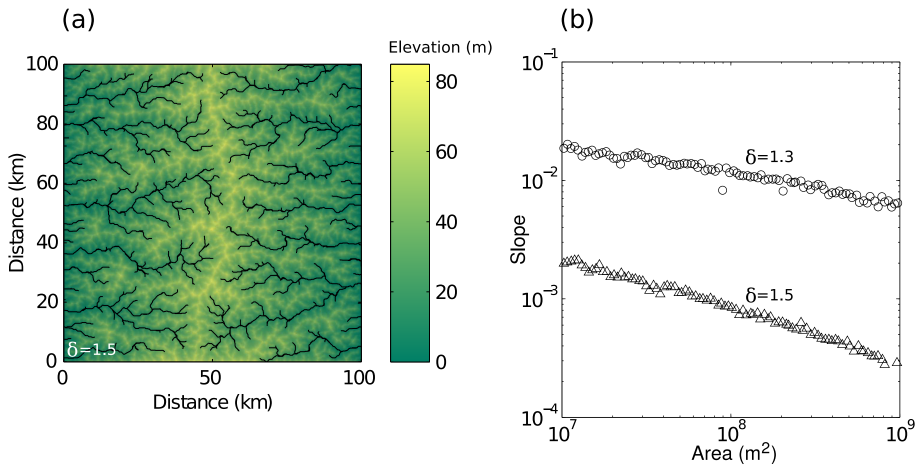

Figure 13. (a) Steady state topography, after 10 Myr, for the sediment transport model where $\delta = 1.5$ and $c = 10^{-4}\,(\mathrm{m}^2\,\mathrm{yr}^{-1})^{1-\delta}$. (b) Slope area relationship for sediment transport model for $\delta = 1.3$ and $\delta = 1.5$.

Table 3. Slope area relationship for trunk streams

sediment transport	k_S	β
$\delta = 1.3$	0.86	-0.23
$\delta = 1.5$	1.76	-0.42
stream power		
$m = 0.3$	0.95	-0.29
$m = 0.5$	6.52	-0.46
$m = 0.7$	71.42	-0.68

for river networks defined by routing water down the steepest slope of descent, the sediment transport model can create catchment morphologies that have a concavity similar to that observed in nature if $\delta \sim 1.5$.

B2 Comparison to Erosion by Stream Power

In order to provide a comparison for the morphology of the sediment transport model we return to the widley used stream power model. We explore how the stream power model evolves to a stead state for a range for the coefficient k and the exponent m.

The landscape derived from the stream power model, equation 6, evolves towards a steady state with a slightly different behaviour in comparison to the sediment transport model (Figure 14). As before we run six models where in this case the first set of three are $m = 0.3$, 0.5 and 0.7 with $k = 10^{-5}\,\mathrm{m}^{-1}\,(\mathrm{m}^2\,\mathrm{yr}^{-1})^{1-\mathrm{m}}$ (Figure 14a). The second set of three are of $m = 0.3$ with $k = 10^{-4}\,\mathrm{m}^{-1}\,(\mathrm{m}^2\,\mathrm{yr}^{-1})^{1-\mathrm{m}}$, $m = 0.5$ with $k = 10^{-5}\,\mathrm{m}^{-1}\,(\mathrm{m}^2\,\mathrm{yr}^{-1})^{1-\mathrm{m}}$, and $m = 0.7$ with $k = 10^{-6}\,\mathrm{m}^{-1}\,(\mathrm{m}^2\,\mathrm{yr}^{-1})^{1-\mathrm{m}}$ (Figure 14b). This range of m is chosen as it spans the range of observed concavities within catchments. As with the sediment

Earth Surf. Dynam. Discuss., doi:10.5194/esurf-2017-34, 2017
Manuscript under review for journal Earth Surf. Dynam.
Discussion started: 19 May 2017

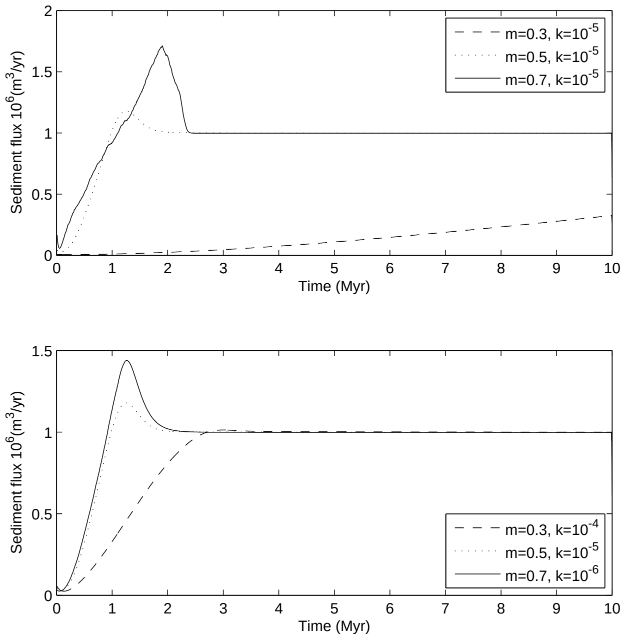

Figure 14. Sediment flux out of the model domain for the sediment transport model for models where (a) $m = 0.3$, 0.5 and 0.7, and $k = 10^{-5}\,(\mathrm{m}^2\,\mathrm{yr}^{-1})^{1-\mathrm{m}}$, and (b) $m = 0.3$, 0.5 and 0.7, and $k = 10^{-4}$, 10^{-5}, and $10^{-6}\,\mathrm{m}^{-1}\,(\mathrm{m}^2\,\mathrm{yr}^{-1})^{1-\mathrm{m}}$.

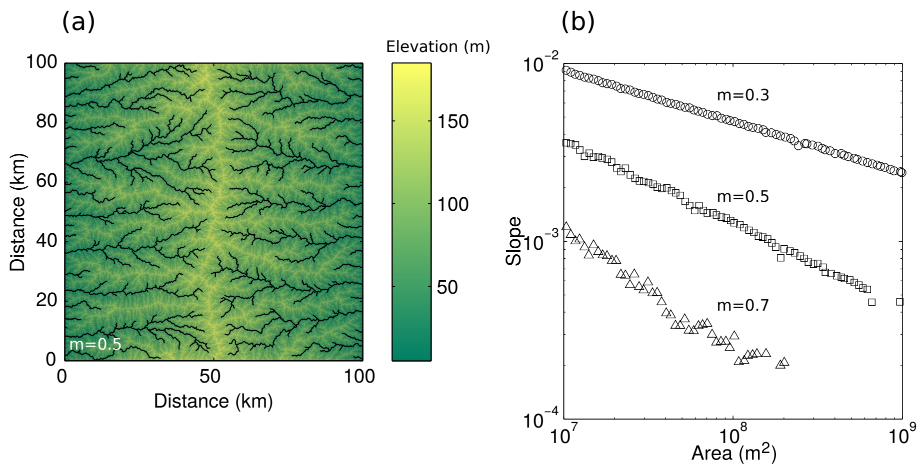

Figure 15. (a) Steady state topography, after 10 Myr, for the sediment transport model where $m = 0.5$ and $k = 10^{-5}\,\mathrm{m}^{-1}\,(\mathrm{m}^2\,\mathrm{yr}^{-1})^{1-\mathrm{m}}$. (b) Slope area relationship for sediment transport model for $m = 0.3$, 0.5 and 0.7.

transport model the coefficient k can be adjusted along with m as they are related, where increasing k reduces the model wind-up time (Figure 14). Decreasing the exponent m increases the timescale taken to reach a steady state (Figure 14)a, however by varying k by a factor of 100 steady state the sediment flux is reached withn 3 Myrs for the three values of m (Figure 14)b.

Following the previous examples, we analyze the topography for the relationship between trunk river slope and drainage area, Figure 15. Both the sediment transport model and the stream power model can create landscapes with similar slope-area realtionships (Table 3). For both models, the value of the intercept k_s and the gradient β are of similar magnitudes. Absolute elevation for the model shown in Figure 15a is higher than the transport limited example due to the larger value of k relative to c. However, importantly, both models can create similar landscape morphologies at steady state.

Acknowledgements. This work initiated under funding by the Royal Astronomical Society through a research fellowship awarded to John Armitage while he was at Royal Holloway University of London. We thank Tom Dunkley Jones (University of Birmingham) for discussions on the duration of conglomeratic deposition duing the PETM, Gareth Roberts (Imperial College London) for discussions on slope exponents and Jean Braun (GFZ Potsdam) for sharing his numerical model Fastscape.

References

Allen, P. A., Armitage, J. J., Carter, A., Duller, R. A., Michael, N. A., Sinclair, H. D., Whitchurch, A. L., and Whittaker, A. C.: The Q_s problem: Sediment volumetric balance of proximal foreland basin systems, Sedimentology, 60, 102–130, doi: 10.1111/sed.12015, 2013.

Armitage, J. J., Duller, R. A., Whittaker, A. C., and Allen, P. A.: Transformation of tectonic and climatic signals from source to sedimentary archive, Nature Geoscience, 4, 231–235, doi: 10.1038/ngeo1087, 2011.

Armitage, J. J., Dunkley Jones, T., Duller, R. A., Whittaker, A. C., and Allen, P. A.: Temporal buffering of climate-driven sediment flux cycles by transient catchment response, Earth and Planetary Science Letters, 369-370, 200–210, doi: 10.1016/j.epsl.2013.03.020, 2013.

Armitage, J. J., Allen, P. A., Burgess, P. M., Hampson, G. J., Whittaker, A. C., Duller, R. A., and Michael, N. A.: Physical stratigraphic model for the Eocene Escanilla sediment routing system: Implications for the uniqueness of sequence stratigraphic architectures, Journal of Sedimentary Research, 85, 1510–1524, doi: 10.2110/jsr.2015.97, 2015.

Baldwin, J. A., Whipple, K. X., and Tucker, G. E.: Implications of the shear stress river incision model for the timescale of postorogenic decay of topography, Journal of Geophysical Research, 108, doi: 10.1029/2011JB000550, 2003.

Banavar, J. R., Colaiori, F., Flammini, A., Giacometi, A., MAritan, A., and Rinaldo, A.: Sculpting of a fractal river basin, Physical Review Letters, 23, 4522–4525, 1997.

Baynes, E. R. C., Attal, M., Niedermann, S., Kirstein, L., Dugmore, A. J., and Naylor, M.: Erosion during extreme flood events dominates Holocene canyon evolution in northeast Iceland, Proceedings of the National Academy of Science, 112, 2355–2360, doi: 10.1073/pnas.1415443112, 2015.

Bonnet, S. and Crave, A.: Landscape response to climate change: Insights from experimental modeling and implications for tectonic versus climatic uplift of topograph, Geology, 31, 123–126, 2003.

Bonnet, S. and Crave, A.: Macroscale dynamics of experimental landscapes, in: Analogue and Numerical Modelling of Crustal-Scale Processes, edited by Buiter, S. J. H. and Schreurs, G., vol. 253 of *Gological Society, London, Special Publications*, pp. 327–339, Geological Society of London, 2006.

Bowen, G. J., Koch, P. L., Cingerich, P. D., Norris, R. D., Bains, S., and Corfield, R. M.: Refined isotope stratigraphy across hte continental Paleocene-Eocene boundary on polecat bench in the Northern Bighorn Basin, in: Paleocene-Eocene Stratigraphy and Biotic Change in the Bighorn and Clark Fork Basins, Wyoming, edited by Gingerich, P. D., vol. 33 of *University of Michigan Papers on Paleontology*, pp. 73–88, University of Michigan, Ann Arbor, Michigan, USA, 2001.

Braun, J. and Willett, S. D.: A very efficient $O(n)$, implicit and parallel method to solve the stream power equation governing fluvial incision and landscape evolution, Geomorphology, 180-181, 170–179, doi: 10.1016/j.geomorph.2012.10.008, 2013.

Braun, J., Voisin, C., Gourlan, A. T., and Chauvel, C.: Erosional response of an actively uplifting mountain belt to cyclic rainfall variations, Earth Surface Dynamics, 3, 1–14, doi: 10.5194/esurf-3-1-2015, 2015.

Campforts, B. and Covers, G.: Keeping the edge: A numerical method that avoids knickpoint smearing when solving the stream power law, Journal of Geophysical Research, 120, 1189–1205, doi: 10.1002/2014JF003376, 2015.

Croissant, T. and Braun, J.: Constraining the stream power law: a novel approach combining a landscape evolution model and an inversion method, Earth Surface Dynamics, 2, 155–166, doi: 10.5194/esurf-2-155-2014, 2014.

Crosby, B. T., Whipple, K. X., Gasparini, N. M., and Wobus, C. W.: Formation of fluvial hanging valleys: Theory and simulation, Journal of Geophysical Research, 112, doi: 10.1029/2006JF000566, 2007.

D'Arcy, M., Whittaker, A. C., and Roda-Boluda, D. C.: Measuring alluvial fan sensitivity to past climate changes using a self-similarity approach to grain-size fining, Death Valley, California, Sedimentology, 64, 388–424, doi: 10.1111/sed.12308, 2016.

Dietrich, W. E., Bellugi, D. G., Sklar, L. S., Srock, J. D., Heimsath, A. M., and Roering, J. J.: Geomorphic transport laws for predicting landscape form and dynamics, in: Prediction in Geomorphology, edited by Wilcock, P. R. and Iverson, R. M., vol. 135 of *Geophysical Monograph*, pp. 1–30, American Geophysical Union, doi: 10.1029/135GM09, 2003.

Dietrich, W. M.: Settling velocity of natural particles, Water Resources Research, 18, 1615–1626, 1982.

Dodds, P. S. and Rothman, D. H.: Geometry of river networks. I. Scaling, fluctuations and deviations, Physical Review E, 63, doi: 10.1103/PhysRevE.63.016115, 2000.

Dunkley Jones, T., Ridgwell, A., Lunt, D. J., Maslin, M. A., Schmidt, D. N., and Valdes, P. J.: A Palaeogene perspective on climate sensitivity and methane hydrate instability, Philisophical transactions of the Royal Society A, 368, 2395–2415, doi: 10.1098/rsta.2010.0053, 2010.

Foreman, B. Z.: Climate-driven generation of a fluvial sheet sand body at the Paleocene–Eocene boundary in north-west Wyoming (USA), Basin Research, 26, 225–241, doi: 10.1111/bre.12027, 2014.

Foreman, B. Z., Heller, P. L., and Clementz, M. T.: Fluvial response to abrupt global warming at the Palaeocene/Eocene boundary, Nature, 491, 92–95, doi: 10.1038/nature11513, 2012.

Ganti, V., Lamb, M. P., and McElroy, B.: Quantitative bounds on morphodynamics and implications for reading the sedimentary record, Nature Comunications, 5, doi: 10.1038/ncomms4298, 2014.

Godard, V., Tucker, G. E., Burch Fisher, G., Burkbank, D. W., and Bookhagen, B.: Frequency-dependent landscape response to climatic forcing, Geophysical Research Letters, 40, 859–863, doi: 10.1002/grl.50253, 2013.

Goren, L.: A theoretical model for fluvial channel response time during time-dependent climatic and tectonic forcing and its inverse applications, Geophysical Research Letters, 43, 10 753–10 763, doi: 10.1002/2016GL070451, 2016.

Grimaud, J. L., Chardon, D., and Beauvais, A.: Very long-term incision of big rivers, Earth and Planetary Science Letters, 405, 74–84, doi: 10.1016/j.epsl.2014.08.021, 2014.

Grimaud, J. L., Paola, C., and Voller, V.: Experimental migration of knickpoints: influence of style of base-level fall and bed lithology, Earth Surface Dynamics, 4, 11–23, doi: 10.5194/esurf-4-11-2016, 2016.

Guerit, L., Métivier, F., Devauchelle, O., Lajeunesse, E., and Barrier, L.: Laboratory alluvial fans in one dimension, Physical Review E, 90, doi: 10.1103/PhysRevE.90.022203, 2014.

Hack, J. T.: Studies of longitudingal profiles in Virginia and Maryland, U.S. Geological Survey Proffesional Papaer, 294-B, 1957.

Hancock, G. R., Coulthard, T. J., and Lowry, J. B. C.: Predicting uncertainty in sediment transport and landscape evolution - the influence of initial surface conditions, Computers and Geosciences, 90, 117–130, doi: 10.1016/j.cageo.2015.08.014, 2016.

Harel, M., Mudd, S. M., and Attal, M.: Global analysis of the stream power law parameters based on worldwide ^{10}Be denudation rates, Geomorphology, 268, 184–196, doi: 10.1016/j.geomorph.2016.05.035, 2016.

Howard, A. D. and Kerby, G.: Channel changes in badlands, Geological Society of America Bulletin, 94, 739–752, 1983.

Izumi, N. and Parker, G.: Inception of channelization and drainage basin formation: upstream-driven theory, Journal of Fluid Mechanics, 283, 341–363, 1995.

Kirkby, M. J.: Hillslope process-response models based on the continuity equation, Special Publication Institute of British Geographers, 3, 15–30, 1971.

Lacey, G.: Stable channels in alluvium, in: Minutes of the Proceedings, edited by Grierson, W. W., vol. 229, pp. 259–292, Institution of Civil Engineers Publishing, 1930.

Lague, D.: The stream power river incision model: evidence, theory and beyond, Earth Surface Processes and Landforms, 39, 38–61, doi: 10.1002/esp.3462, 2014.

Leopold, L. B. and Maddock, T.: The hydraulic geometry of stream channels and some physiographic implications, Tech. Rep. 252, U.S. Geological Survey Proffesional Papers, 57 p., 1953.

Liu, Y., Métivier, F., Gaillerdet, J., Ye, B., Meunier, P., Narteau, C., Lajeunesse, E., Han, T., and Malverti, L.: Erosion rates deduced from seasonal mass balance along the upper Urumqi River in Tianshan, Solid Earth, 2, 283–301, doi: 10.5194/se-2-283-2011, 2011.

Manners, H. R., Grimes, S. T., Sutton, P. A., Domingo, L., Leng, M. J., Twitchett, R. J., Hart, M. B., Dunkley Jones, T., Pancost, R. D., Duller, R., and Lopez-Martinez, N.: Magnitude and profile of organic carbon isotope records from the Paleocene - Eocene Thermal Maximum: Evidence from northern Spain, Earth and Planetary Science Letters, 376, 220–230, doi: 10.1016/j.epsl.2013.06.016, 2013.

Maritan, A., Rinaldo, A., Rigon, R., Giacometti, A., and Rordriguez-Iturbe, I.: Scaling laws for river networks, Physical Review E, 53, 1510–1515, 1996.

Meunier, P., Métivier, F., Lajeunesse, E., Mériaux, A. S., and Faure, J.: Flow pattern and sediment transport in a braided river: The "torrent de St Pierre" (French Alps), Journal of Hydrology, 330, 496–505, doi: 10.1016/j.jhydrol.2006.04.009, 2006.

Michael, N. A., Whittaker, A. C., Carter, A., and Allen, P. A.: Volumetric budget and grain-size fractionation of a geological sediment routing system: Eocene Escanilla Formation, south-central Pyrenees, Geological Society of America Bulletin, 126, 585–599, doi: 10.1130/B30954.1, 2014.

Paola, C., Heller, P. L., and Angevine, C. L.: The large-scale dynamics of grain-size variation in alluvial basins, 1: Theory, Basin Research, 4, 73–90, doi: 10.1111/j.1365-2117.1992.tb00145.x, 1992.

Pastor-Satorras, R. and Rothman, D. H.: Stochastic Equation for the Erosion of Inclined Topography, Physical Review Letters, 80, 4349–4352, doi: 10.1103/PhysRevLett.80.4349, 1998.

Perron, J. T. and Royden, L.: An integral approach to bedrock river profile analysis, Earth Surface Processes and Landforms, 38, 570–576, doi: 10.1002/esp.3302, 2012.

Pritchard, D., Roberts, G. G., White, N. J., and Richardson, C. N.: Uplift histories from river profiles, Geophysical Research Letters, 36, doi: 10.1029/2009GL040928, 2009.

Rigon, R., Rodriguez-Iturbe, I., Maritan, A., Giacometti, A., Tarboton, D. G., and Rinaldo, A.: On Hack's law, Water Resources Research, 32, 3367–3374, 1996.

Roberts, G. G. and White, N.: Estimating uplift rate histories from river profiles using African examples, Journal of Geophysical Research, 115, doi: 10.1029/2009JB006692, 2010.

Rohais, S., Bonnet, S., and Eschard, R.: Sedimentary record of tectonic and climatic erosional perturbations in an experimental coupled catchment-fan system, Basin Research, 23, 1–15, doi: 10.1111/j.1365-2117.2011.00520.x, 2011.

Röhl, U., Westerhold, T., Bralower, T. J., and Zachos, J. C.: On the duration of the Paleocene-Eocene thermal maximum (PETM), Geochemistry, Geophysics, Geosystems, 8, doi: 10.1029/2007GC001784, 2007.

Roy, S. G., Koons, P. O., Upton, P., and Tucker, G. E.: The influence of crustal strength fields on the patterns and rates of fluvial incision, Journal of Geophysical Research, 120, 275–299, doi: 10.1002/2014JF003281, 2015.

Rudge, J. F., Roberts, G. G., White, N. J., and Richardson, C. N.: Uplift histories of Africa and Australia from linear inverse modeling of drainage inventories, Journal of Geophysical Research, 120, 894–914, doi: 10.1002/2014JF003297, 2015.

Schmitz, B. and Pujalte, V.: Abrupt increase in seasonal extreme precipitation at the Paleocene-Eocene boundary, Geology, 35, 215–218, doi: 10.1130/G23261A.1, 2007.

Earth Surf. Dynam. Discuss., doi:10.5194/esurf-2017-34, 2017
Manuscript under review for journal Earth Surf. Dynam.
Discussion started: 19 May 2017

Schwanghart, W. and Scherler, D.: Short Communication: TopoToolbox 2–MATLAB-based software for topographic analysis and modeling in Earth surface sciences, Earth Surface Dynamics, 2, 1–7, doi: 10.5194/esurf-2-1-2014, 2014.

Simpson, G. and Schlunegger, F.: Topographic evolution and morphology of surfaces evolving in response to coupled fluvial and hillslope sediment transport, Journal of Geophysical Research, 108, doi: 10.1029/2002JB002162, 2003.

Singh, A., Reinhardt, L., and Foufoula-Georgiou, E.: Landscape reorganization under changing climatic forcing: Results from an experimental landscape, Water Resources Research, 51, 4320–4337, doi: 10.1002/2015WR017161, 2015.

Sluijs, A., Schouten, S., Pagani, M., Woltering, M., Brinkhuis, H., Sinninghe Damsté, J. S., Dickens, G. R., Huber, M., Reichart, G. J., Stein, R., Matthiessen, J., Lourens, L. J., Pedentchouk, N., Backman, J., Moran, K., and the Expedition 302 scientists: Subtropical Arctic Ocean temperatures during the Palaeocene/Eocene thermal maximum, Nature, 411, 610–613, doi: 10.1038/nature04668, 2006.

Smith, T. R.: A theory for the emergence of channelized drainage, Journal of Geophysical Research, 115, doi: 10.1029/2008JF001114, 2010.

Smith, T. R. and Bretherton, F. P.: Stability and conservation of mass in drainage basin evolution, Water Resources Research, 8, 1506–1529, doi: 10.1029/WR008i006p01506, 1972.

Smith, T. R., Merchant, G. E., and Birnir, B.: Transient attractors: towards a theory of the graded stream for alluvial and bedrock channels, Computers and Geosciences, 26, 541–580, doi: 10.1016/S0098-3004(99)00128-4, 2000.

Snyder, N. P., Whipple, K. X., Tucker, E., and Merrits, D. J.: Landscape response to tectonic forcing: Digital elevation model analysis of stream profiles in the Mendocino triple junction region, northern California, Geological Society of America Bulletin, 112, 1250–1263, doi: 10.1130/0016-7606(2000)112<1250:LRTTFD>2.0.CO;2, 2000.

Tarboton, D. G., Bras, R. L., and Rodriguez-Iturbe, I.: Comment on “On the fractal dimension of stream network” by Paolo La Barbera and Renzo Rosso, Water Resources Research, 26, 2243–2244, doi: 10.1029/WR026i009p02243, 1990.

Temme, A. J. A. M., Armitage, J. J., Attal, M., and van Gorp, W.: Choosing and using landscape evolution models to inform field stratigraphy and landscape reconstruction studies, Earth Surface Processes and Landforms, doi: 10.1002/esp.4162, 2017.

Tinkler, K. J. and Whol, E. E.: Rivers over Rock: fluvial processes in bedrock channels, Geophysical Monograph Series; 107, American Geophysical Union, Washington, USA, 1998.

Tucker, G. E. and Whipple, K. X.: Topographic outcomes predicted by stream erosion models: Sensitivity analysis and intermodel comparison, Journal of Geophysical Research, 107, doi: 10.1029/2001JB000162, 2002.

Valla, P. G., van der Beek, P. A., and Lague, D.: Fluvial incision into bedrock: Insights from morphometric analysis and numerical modeling of gorges incising glacial hanging valleys (Western Alps, France), Journal of Geophysical Research, 116, doi: 10.1029/2008JF001079, 2010.

van der Beek, P. and Bishop, P.: Ceonzoic river profile development in the Upper Lachlan catchment (SE Australia) as a test of quantative fluvial incision models, Journal of Geophysical Research, 108, doi: 10.1029/2002JB002125, 2003.

Whipple, K. X.: Fluvial landscape response time: how plausible is steady-state denudation, American Journal of Science, 301, 313–325, 2001.

Whipple, K. X.: Bedrock rivers and the geomorphology of active orogens, Annual Reviews of Earth and Planetary Science, 32, 151–185, doi: 10.1146/annurev.earth.32.101802.120356, 2004.

Whipple, K. X. and Meade, B. J.: Orogen response to changes in climatic and tectonic forcing, Earth and Planetary Science Letters, 243, 218–228, doi: 10.1016/j.epsl.2005.12.022, 2006.

Whipple, K. X. and Tucker, G. E.: Dynamics of the strea-power river incision model: Implications for height limits of mountain ranges, landscape response times, and research needs, Journal of Geophysical Research, 104, 17 661–17 674, 1999.

Whipple, K. X. and Tucker, G. E.: Implications of sediment-flux-dependent river incision models for landscape evolution, Journal of Geophysical Research, 107, doi: 10.1029/2000JB000044, 2002.

Whittaker, A. C. and Boulton, S. J.: Tectonic and climatic controls onknickpoint retreat rates and landscapre response times, Journal of Geophyscial Research, 117, doi: 10.1029/2011JF002157, 2012.

Whittaker, A. C., Cowie, P. A., Attal, M., Tucker, G. E., and Roberts, G. P.: Bedrock channel adjustment to tectonic forcing: Implications for predicting river incision rates, Geology, 35, 103–106, doi: 10.1130/G23106A.1, 2007.

Whittaker, A. C., Attal, M., Cowie, P. A., Tucker, G. E., and Roberts, G.: Decoding temporal and spatial patterns of fault uplift using transient river long-profiles, Geomorphology, 100, 506–526, doi: 10.1016/j.geomorph.2008.01.018, 2008.

Whittaker, A. C., Duller, R. A., Springett, J., Smithells, R. A., Whitchurch, A. L., and Allen, P. A.: Decoding downstream trends in stratigraphic grain size as a function of tectonic subsidence and sediment supply, Geological Society of America Bulletin, 123, 1363–1382, 2011.

Willett, S. D., McCoy, S. W., Perron, J. T., Goren, L., and Chen, C.: Dynamic Reorganization of River Basins, Science, 343, doi: 10.1126/science.1248765, 2014.

Willgoose, G., Bras, R. L., and Rodriguez-Iturbe, I.: A physical explanation of an observed link area-slope relationship, Water Resources Research, 27, 1697–1702, 1991.

Wobus, C., Whipple, K. X., Kirby, E., Snyder, N., Johnson, J., Spyropolou, K., Crosby, B., and Sheehan, D.: Tectonics from topography: Procedures, promise, and pitfalls, Geological Society of America Special Papers, 398, 55–74, 2006.

Wobus, C. W., Tucker, G. E., and Anderson, R. S.: Does climate change create distinctive patters of landscape incision?, Journal of Geophysical Research, 115, doi: 10.1029/2009JF001562, 2010.